Advances in sustainable fluorine-free CSD $YBa_2Cu_3O_7$ thin films

Pieter Vermeir[1,2], Jonas Feys[2], Glenn Pollefeyt[2], Bram Verslyppe[1], Asha De Brabandere[1], Kim Verbeken[3], Michael Bäcker[4], Petra Lommens[2], Joseph Schaubroeck[1], Klaartje De Buysser[2] and Isabel Van Driessche[2]
[1]University College Ghent, Faculty of Applied Engineering sciences, Belgium.
[2] Ghent University, Department of Inorganic and physical chemistry, Belgium.
[3] Ghent University, Department of Materials Science and Engineering, Belgium.
[4] Deutsche Nanoschicht, Germany.

ABSTRACT

Chemical solution deposition techniques are a very competitive low cost method to achieve coated conductors. Recently, fluorine-free CSD methods have made a great progress for the preparation of YBCO thin films and became a sustainable alternative for the well-known trifluoroacetate CSD approach. By elucidating the reaction mechanism behind this new approach, finally giving an answer to the question why it is possible to fabricate YBCO films without TFA, different processing routes were discovered giving rise to high superconducting YBCO films (>1MA.cm^{-2}). Each route has it's own benefits. One specific route offers the opportunity to tune the crystallographic orientation. By changing one process parameter, a shift from complete c-axis to complete a-axis orientation is observed. This can be very useful for e.g. Josephson Junctions.

We particularly investigated the fundamental reaction mechanism of each reaction route, with the focus on the corresponding barium compound. Although good superconducting properties are obtained, still one major drawback limits industrial implementation: thickness. It is observed that a critical thickness of ~500 nm eliminates the superconducting properties. Therefore, this paper gives a summary of all progress made regarding to fluorine-free water-based CSD YBCO thin films with emphasis on the possibility to control the crystallization rate.

INTRODUCTION

Since the discovery of the so-called high-temperature superconductors, cheap liquid nitrogen (77K) could be used as a cooling agent raising the economical feasibility of many applications to a realistic level [1]. A major application territory is the production of superconducting cables enabling heat losses during transportation of current [2]. Currently, all high-temperature superconductors are ceramic materials which are inherently very brittle of nature. When used as bulk material, this characteristic hampers easy operability within practical cable applications (flexibility). To overcome this difficulty, coated conductors were introduced [3,4]. A coated conductor is a composition of a thin superconducting layer deposited on a flexible substrate template. For coated conductor designs, the most promising high-temperature superconducting ceramic is $YBa_2Cu_3O_7$ (YBCO) [5].

The most common techniques to deposit YBCO on the substrate template require expensive vacuum equipment and are limited in production speed [6]. An alternative for this vacuum technology lies in synthesizing a layer by coating a metal-containing precursor solution onto the substrate template. A subsequent thermal process transforms the coated layer into a superconducting solid phase. This method, overall classified as Chemical Solution Deposition

(CSD), has much lower investment and operational costs in addition to higher deposition speeds [7]. Within the CSD environment, different coating technologies for long length applications are present including dip coating and ink jet printing [8]. The low precursor consumption and the ability of patterning are the main advantages of ink-jet printing, while dip coating is the most simple up-scalable technology.

Amongst the different CSD precursor designs described for the synthesis of YBCO, metalorganic deposition using trifluororacetates (TFA) is the most conventional [5,9-11]. However, this method's main drawbacks are the long processing times reducing the economical feasibility as well as the possible HF release during processing. Therefore, two new approaches are appearing in this research field: (i) low fluorine containing precursors to reduce the HF release and processing time and (ii) fluorine-free precursors leading to the elimination of HF. Within this work, the advances made for fluorine-free CSD precursors using water as primary solvent are reviewed and judged towards industrial feasibility.

EXPERIMENT

The fluorine-free CSD precursor was prepared using metal-acetates, water, acetic acid and tri-ethanolamine. Details concerning the preparation method of the precursor and complexation behavior of the corresponding species are reported elsewhere [12,13]. This solution was dip coated on $SrTiO_3$ (STO) single crystal substrates using a computer-controlled precision dip coater. All coating procedures were performed in a dedicated class 10000 clean room to avoid dust contamination. Using a single dip at a withdrawal speed of 20-50 mm min^{-1}, YBCO precursor films on STO substrates were prepared.

Thermogravimetric analysis (TGA) experiments were performed using a Stanton-Redcroft STA 1500 set-up. Powder mixtures were ball-milled for 12 h to ensure a homogeneous mixture of small grains. Powders of different metal combinations were mixed in a metal-ratio referring to the stoichiometry in YBCO.

HT-XRD (high temperature X-ray diffraction) measurements were performed using a Bruker D8 discover set-up using a parallel beam geometry in a θ-2θ position with a Si(Li) detector.

DISCUSSION

An important issue in process optimization is contained in gathering knowledge of the underlying mechanism. Consequently, the elucidation of the reaction mechanism was the primary breakthrough for process adjustments. Using TGA-DTA experiments in bulk and HT-XRD data in thin film analysis, we were able to identify the crucial role of $BaCO_3$ in a three step YBCO formation mechanism [14]. The crucial reaction step is the reduction in decarboxylation temperature of $BaCO_3$, intrinsically a very stable compound, in the presence of CuO. It is believed that CuO acts as a catalyst for the decarboxylation. This behavior is clearly observed in TGA experiments, illustrated in Figure 1. XRD analysis of the final product identified the existence of $BaCuO_2$.

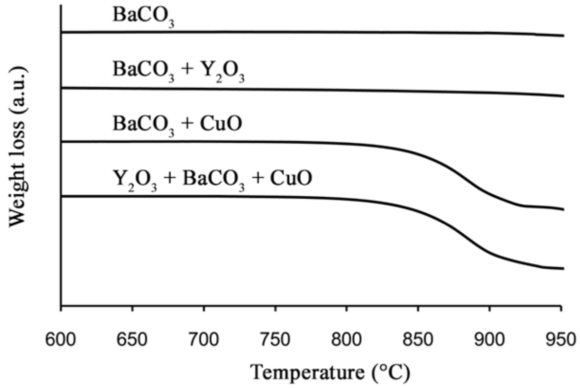

Figure 1. TGA spectra of different species heated at 10°C.min^{-1}.

In a next step, which can occur simultaneously with the previous step, the intermediate $BaCuO_2$ reacts with the remaining CuO to form a liquid. Finally, the liquid will react with Y_2O_3 to crystallize YBCO. Below, the corresponding mechanism is summarized:

$$BaCO_3 + CuO \rightarrow BaCuO_2 + CO_2\uparrow \tag{1}$$
$$2BaCuO_2 + CuO \rightarrow \text{liquid} + O_2\uparrow \tag{2}$$
$$\tfrac{1}{2}Y_2O_3 + \text{liquid} \rightarrow YBa_2Cu_3O_{6+x} \tag{3}$$

Knowing the reaction mechanism, the link between all reaction steps and the corresponding thermal process could be identified. Within a standard heating process, 5 different stages are observed: (A) amorphous solution coated film (B) burnout of the organic precursors (C) $BaCuO_2$ and liquid phase formation (D) YBCO nucleation and (E) YBCO growth (Figure 2). Depending on processing parameters, stages can overlap, be eliminated or extended.

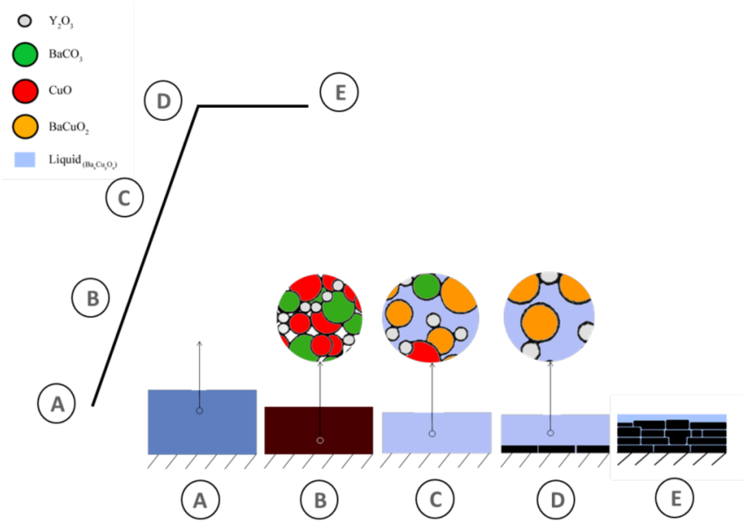

Figure 2. Link between reaction mechanism and thermal treatment

A significant parameter within the thermal process is the sinter temperature. Using the link between the partial oxygen versus temperature diagram and YBCO formation reactions, it is observed that epitaxial YBCO films were produced when sintering took place at a temperature above the fully binairy liquidus temperature T_l (where the binary reaction between $BaCO_3$ and CuO results in a complete liquid phase) and below the peritectic temperature T_{pl} (where YBCO can react peritectically with CuO to form Y_2BaCuO_5). Using a heating rate of $5°C.min^{-1}$, at a sinter temperature of 815°C in a partial oxygen pressure of 200 ppm mixed with nitrogen, a c-axis oriented YBCO film with a $T_{c,onset}$ of 92 K, ΔT_c of 2 K and a J_c of 1.1 $MA.cm^{-2}$ was obtained. For a 450 nm thick film, this resulted in an I_c of 50 A/cm-width. During all experiments, it was noticed that I_c dropped to zero as soon as a critical thickness of around 500 nm was exceeded.

Extending stage B, by introducing a burnout at 400°C under O_2 to enhance complete combustion, resulted remarkably in complete a-axis orientation of the YBCO film [15]. This result indicated that YBCO nucleation occurred at low temperatures, giving preferential a-axis orientation. The latter is confirmed by literature. Therefore, YBCO nucleation should be blocked in this critical temperature interval to avoid a-axis nucleation and growth. Taking into account the reaction mechanism, YBCO formation (reaction 3) can be stopped by blocking reaction 1. Conform Le Chatelier’s principle, the introduction of a partial CO_2 pressure should be able to withstand $BaCuO_2$ formation and consequently YBCO formation. By introducing 10 vol% of CO_2 in the heating atmosphere after a preceding burnout (extended stage B), the nucleation temperature can be controlled. Releasing the CO_2 introduction at 815°C results in a complete c-axis oriented YBCO film. A $T_{c,onset}$ of 92 K, ΔT_c of 2 K and a J_c of 1.25 $MA.cm^{-2}$ was obtained. Using this specific route, we were able to tune the superconducting properties. As different applications require different orientations (e.g. josephson junctions require a-axis orientation while current transportation requires c-axis orientation) this method shows a high flexibility for multiple application fields. Nevertheless, it was once again noted that J_c dropped to zero when exceeding a critical thickness of ~500 nm.

Both reaction routes, with and without burnout, indicate a limitation in layer thickness. We presume that the high crystallization rates of this fluorine-free approach are limiting further development. In order to follow the crystallization process, a HT-XRD experiment was set-up. A layer containing Y_2O_3, $BaCO_3$ and CuO in a Y/Ba/Cu ratio of 1/2/3 was heated until 900°C at a heating rate of $10°C.min^{-1}$ under a 200 ppm O_2:N_2 mixture (Figure 3). The layer was prepared by dip coating the precursor described in the experimental part on a STO substrate, follow by a burnout process at 500°C in O_2.

Following the (005)-reflection of YBCO at a 2θ of 38.5°, we can see from the intensity change during heating that YBCO crystallization is extremely fast for this fluorine-free approach. For TFA-related methods, crystallization rates are controlled by the partial water vapor pressure. In order to overcome this bottleneck for fluorine-free CSD methods, a control in crystallization rate needs to be found. One suggestion could be a controlled release of CO_2 in the CO_2-assisted processing route, as nucleation and growth of YBCO is indirectly connected with the formation of $BaCuO_2$ of reaction 1.

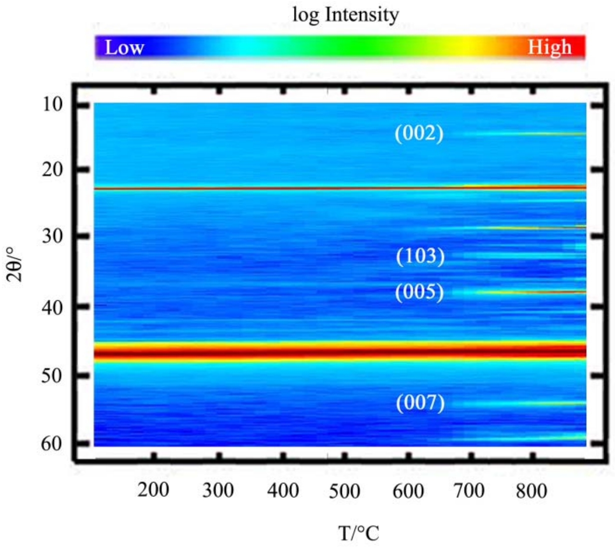

Figure 3. HT-XRD measurement of a Y_2O_3-$BaCO_3$-CuO film under a 200 ppm O_2:N_2 atmosphere with a heating ramp of 10°C.min^{-1}.

CONCLUSIONS

By elucidating the reaction mechanism of fluorine-free water-based CSD processes in YBCO formation, different reaction routes were discovered. In one specific route, we were able to tune the superconducting properties by changing one single process parameter, resulting in a high flexibility for multiple application fields. Nevertheless, a critical thickness borderline of ~500 nm is observed within all reaction routes. For industrial implementation, we need to overcome this bottleneck. We believe that the high crystallization rates during YBCO formation using the fluorine-free approach causes this limitation. This assumption is strengthened by a HT-XRD experiment, where we were able to observe this fast c-axis YBCO crystallization. In order to avoid these issues, a controlled release of CO_2 in the CO_2-adapted process is suggested.

ACKNOWLEDGMENTS

Bart Ruttens is gratefully acknowledged for performing HT-XRD measurements. KimVerbeken is a postdoctoral fellow with the Fund for Scientific Research-Flanders (Belgium) (FWO Vlaanderen).

REFERENCES

1. J.G. Bednorz and K.A. Muller, Z. Phys. B **64**, 2 (1986).
2. M. Bäcker, Z. Kristallogr. **226** (2011).
3. V. Selvamanickam, Y.M. Chen, X.M. Xiong, Y.Y.Y. Xie, M. Martchevski, A. Rar, Y.F. Qiao, R.M. Schmidt, A. Knoll, K.P. Lenseth and C.S. Weber, IEEE Trans. Appl. Supercond. **19**, 3 (2009).

4. G. Pollefeyt, S. Rottiers, P. Vermeir, P. Lommens, R. Hühne, K. De Buysser and I. Van Driessche, J. Mater. Chem. A **1** (2013).
5. P. Vermeir, I. Cardinael, M. Bäcker, J. Schaubroeck, E. Schacht, S. Hoste and I. Van Driessche, Supercond. Sci.Technol. **22** 075009 (2009).
6. I. Van Driessche, G. Penneman, E. Bruneel and S. Hoste, Pure Appl. Chem. **74** (2002).
7. P. Vermeir, F. Deruyck, J. Feys, P. Lommens, J. Schaubroeck and I. Van Driessche, J. Sol-Gel Sci. Technol. **62** (2012).
8. J. Feys, P. Vermeir, P. Lommens, S.C. Hopkins, X. Granados, B.A. Glowacki, M. Bäcker, E. Reich, S. Ricard, B. Holzapfel, P. Van Der Voort and I. Van Driessche, J. Mater. Chem. **22** (2012)
9. X. Obradors, T. Puig, A. Pomar, F. Sandiumenge, N. Mestres, M. Coll, A. Cavallaro, N. Roma, J. Gazquez, J.C. Gonzalez, O. Castano, J. Gutierrez, A. Palau, K. Zalamova, S. Morlens, A. Hassini, M. Gibert, S. Ricart, J.M. Moreto, S. Pinol, D. Isfort and J. Bock, Supercond. Sci. Technol. **19**, 3 (2006).
10. B.A. Albiss and I.M. Obaidat, J. Mater. Chem. **20** (2010).
11. T. Manabe, M. Sohma, I. Yamaguchi, K. Tsudaka, W. Kondo, K. Kamiya, T. Tsuchiya, S. Mizuta, T. Kumagai, Physica C **445** (2006).
12. B. Schoofs, V. Cloet, P. Vermeir, J. Schaubroeck, S. Hoste and I. Van Driessche, Supercond. Sci. Technol. **19**, 11 (2006).
13. B. Schoofs, D. Van de Vyver, P. Vermeir, J. Schaubroeck, S. Hoste, G. Herman and I. Van Driessche, J. Mater. Chem. **17**, 17 (2007).
14. P. Vermeir, I. Cardinael, J. Schaubroeck, K. Verbeken, M. Baecker, P. Lommens, W. Knaepen, J. D’haen, K. De Buysser and I. Van Driessche, Inorg. Chem. **49**, 10 (2010).
15. P. Vermeir, J. Feys, J. Schaubroeck, K. Verbeken, M. Baecker and I. Van Driessche, Mater. Chem. Phys. **133**, 2-3 (2012).